

High-field antiferromagnetic resonance in single-crystalline $\text{La}_{0.95}\text{Sr}_{0.05}\text{MnO}_3$: Experimental evidence for the existence of a canted magnetic structure

A. Pimenov,¹ M. Biberacher,¹ D. Ivannikov,¹ A. Loidl,¹ V. Yu. Ivanov,² A. A. Mukhin,² and A. M. Balbashov³

¹*Experimentalphysik V, EKM, Universität Augsburg, D-86135 Augsburg, Germany*

²*General Physics Institute of the Russian Academy of Sciences, 117942 Moscow, Russia*

³*Moscow Power Engineering Institute, 105835 Moscow, Russia*

(Received 18 May 2000)

High-field antiferromagnetic-resonance (AFMR) spectra were obtained in the frequency range 40 GHz $< \nu < 700$ GHz and for magnetic fields up to 8 T in twin-free single crystals of $\text{La}_{0.95}\text{Sr}_{0.05}\text{MnO}_3$. At low temperatures two antiferromagnetic modes were detected, which reveal different excitation conditions and magnetic field dependencies. No splitting of these modes was observed for any orientation of the static magnetic field excluding the phase-separation scenario for this composition. Instead, the full data set including the anisotropic magnetization can be well described using a two-sublattice model of a canted antiferromagnetic structure.

I. INTRODUCTION

The idea of phase separation in the manganite perovskites ($R_{1-x}M_x\text{MnO}_3$, $R=\text{La, Pr, } \dots$, $M=\text{Ca, Sr, } \dots$) is one of the most controversially discussed topics concerning the electronic properties of these compounds. After the pioneering works of Jonker and van Santen¹ and of Wollan and Koehler,² de Gennes³ developed a model in which the purely antiferromagnetic and insulating LaMnO_3 on increasing doping passes through a canted (CAF) ground state and arrives at a purely ferromagnetic and metallic state at high doping level ($x \geq 0.2$). This phase diagram was calculated using competing superexchange (SE) and double exchange interactions.⁴

However, in recent years a number of theoretical models predicted that the CAF structure becomes unstable against electronic phase separation into ferromagnetic (FM) and antiferromagnetic (AFM) regions.^{5,6} As discussed by Yunoki *et al.*,⁶ the tendency to the phase separation seems to be an intrinsic property of the double-exchange model. A number of experimental data including neutron scattering⁷ and NMR⁸ pointed toward the existence of the phase separation in different types of manganites. For discussion of the recent results see Refs. 6,9.

It has to be pointed out that the experimental observation of electronic phase separation is rather difficult. Already more than forty years ago, Wollan and Koehler² stated that, on the basis of neutron diffraction experiments, it is impossible to decide whether the structure of the doped manganites is homogeneously canted or inhomogeneously mixed FM and AFM. Only a few experimental methods can distinguish between inhomogeneous and homogeneous magnetic phases because the technique has to be sensitive to the local magnetic structure of the sample. In addition, a sample quality appears to be of major importance for these experiments. Antiferromagnetic resonance (AFMR) seems to be an excellent tool for the solution of the phase-separation problem. The main parameters of the resonance lines, such as position, excitation conditions, behavior in magnetic field, etc., sensi-

tively depend on the local environment of the magnetic moments. Recently, using this method, we have investigated the concentration dependence of AFMR lines in low-doped $\text{La}_{1-x}\text{Sr}_x\text{MnO}_3$ without external magnetic field.¹⁰ The results were explained within the frame of a two-sublattice model, which strongly supported the existence of a canted magnetic structure. Most $\text{La}_{1-x}\text{Sr}_x\text{MnO}_3$ crystals of this series were twinned. However, the samples with 5% Sr concentration were identified as untwinned single crystals. This fact allowed the unambiguous determination of the excitation conditions of AFMR lines and to carry out detailed investigations in static magnetic fields. In this paper we present, in addition to the results of the magnetic-field experiments, anisotropic magnetization curves and compare the observed data with the predictions of a two-sublattice model. The possible explanations within phase separation models are also discussed.

II. EXPERIMENTAL DETAILS

$\text{La}_{0.95}\text{Sr}_{0.05}\text{MnO}_3$ single crystals were grown by a floating zone method with radiation heating.¹¹ X-ray powder diffraction measurements showed that the crystals were single-phase. Four-circle x-ray analysis showed the twin-free structure of the crystal. The temperature dependence of the dc resistivity of these samples has been published previously¹² and agrees well with literature data.¹³ Plane-parallel plates of size approximately $8 \times 8 \times 1$ mm³ were used for optical measurements. The magnetic measurements were carried out on small pieces of the same crystals.

The magnetization curves of $\text{La}_{0.95}\text{Sr}_{0.05}\text{MnO}_3$ were measured using a SQUID magnetometer in fields up to 6.5 T. The transmission spectra in the frequency range 40 GHz $\leq \nu \leq 700$ GHz ($1.3 - 23$ cm⁻¹) were recorded using a quasi-optical technique utilizing backward-wave oscillators as coherent light sources.¹⁴ Combining this method with a superconducting split-coil magnet equipped with optical windows allows to carry out transmission experiments in fields up to 8T. The data were obtained in the frequency-sweep mode at constant magnetic field. However, in some cases

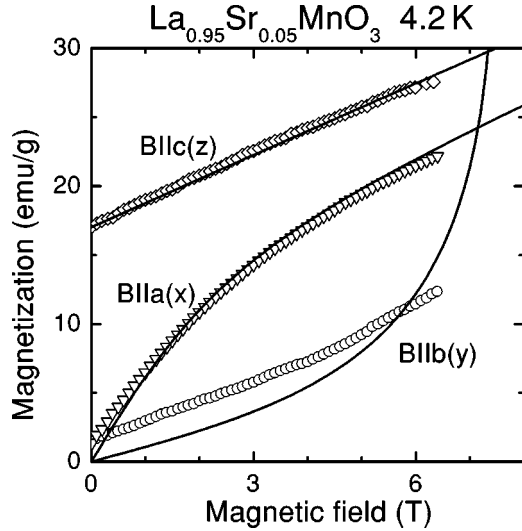


FIG. 1. Magnetization of $\text{La}_{0.95}\text{Sr}_{0.05}\text{MnO}_3$ single crystal along different crystallographic axes at $T=4.2$ K. Symbols represent the experimental data, lines are calculated according to the two-lattice model as described in the text.

field-sweep measurements were performed because this procedure enhances the accuracy of determination of resonance frequencies. The frequency-dependent transmission spectra were analyzed using the Fresnel optical formulas for a transmission coefficient of a plane-parallel plate.¹⁵ The relative transparency of the sample in the frequency range investigated resulted in the observation of interference patterns in the spectra. The observation of these interferences allowed the calculation of the optical parameters of the sample without measuring the phase shift of the transmitted signal. The dispersion of the magnetic permeability was taken into account assuming a harmonic oscillator model for the complex magnetic permeability:

$$\mu^*(\nu) = \mu_1 + i\mu_2 = 1 + \Delta\mu\nu_0^2/(\nu_0^2 - \nu^2 + i\nu g), \quad (1)$$

where ν_0 , $\Delta\mu$, and g are eigenfrequency, mode strength, and width of the resonance, respectively. The dielectric parameters of the sample ($n^* = n + ik$) were assumed to behave regularly in the vicinity of the resonance frequency. Hence, the frequency-sweep measurements allowed to obtain absolute values of the parameters of AFMR lines.

III. RESULTS AND DISCUSSION

Figure 1 shows the low-temperature magnetization curves of single-crystalline $\text{La}_{0.95}\text{Sr}_{0.05}\text{MnO}_3$ for different orientations of the magnetic field. The magnetization along the c axis shows a spontaneous magnetization and therefore is identified as the direction of the weak ferromagnetic moment. The magnetization along the crystallographic b axis reveals the weakest field dependence and thus resembles the data of a simple antiferromagnet along the easy (antiferromagnetic) axis.¹⁶

In order to understand the magnetization measurement and the submillimeter spectra quantitatively, a two-sublattice model has been adopted. The two-sublattice model is a widely used approximation to describe the properties of magnetically ordered materials.¹⁷ It was originally applied to

the spin-wave spectrum of manganites by de Gennes.³ For a realistic description, additional contributions to the free energy, i.e., the single ion anisotropy $D_x\sum_i S_{xi}^2 + D_z\sum_i S_{zi}^2$ and the Dzyaloshinsky-Moria (DM) antisymmetric exchange interactions $\sum_{i,j} \mathbf{d}_{ij}[S_i S_j]$ have to be taken into account. In the classical approximation the free energy at $T=0$ is given by

$$F(\mathbf{m}, \mathbf{l}) = \frac{1}{2} A \mathbf{m}^2 - B |\mathbf{m}| + \frac{1}{2} K_x (m_x^2 + l_x^2) + \frac{1}{2} K_z (m_z^2 + l_z^2) - d(m_z l_y - m_y l_z) - M_0 \mathbf{m} \mathbf{H}. \quad (2)$$

In Eq. (2) the (x, y, z) axes of the coordinate system are directed along the crystallographic axes (a, b, c) of the sample ($a=5.547$ Å, $b=5.666$ Å, $c=7.725$ Å). The first and the second terms of Eq. (2) describe antiferromagnetic and ferromagnetic (double) exchange, the third and fourth terms give the single ion anisotropy, the fifth term describes the DM exchange while the last term takes into account effects of an external magnetic field. In Eq. (2), \mathbf{m} and \mathbf{l} are dimensionless ferro- and antiferromagnetic vectors, which are defined as $\mathbf{m} = (\mathbf{M}_1 + \mathbf{M}_2)/2M_0$, $\mathbf{l} = (\mathbf{M}_1 - \mathbf{M}_2)/2M_0$ and satisfy the conditions $\mathbf{m} \mathbf{l} = 0$, $\mathbf{m}^2 + \mathbf{l}^2 = 1$ since the sublattices \mathbf{M}_1 and \mathbf{M}_2 are assumed to be saturated at $T=0$. The parameter B describes the DE interaction. $K_{x,z} > 0$ are anisotropy constants stabilizing the $A_y F_z$ configuration in pure LaMnO_3 . d is the interlayer antisymmetric exchange constant. $M_0 = 0.95M_0(\text{Mn}^{3+}) + 0.05M_0(\text{Mn}^{4+}) = 3.95\mu_B$, is the saturation magnetization of the sublattices. The equilibrium arrangement of the sublattices has been obtained minimizing the free energy given by Eq. (2). The frequencies of the resonance modes were calculated in the limit of small perturbations from the equations of motion $d\mathbf{M}_i/dt = \gamma[\mathbf{M}_i \times \partial F/\partial \mathbf{M}_i]$, ($i=1,2$), where γ is the gyro-magnetic ratio.

The solutions of Eq. (2) for the $\mathbf{H}||c$ were published previously.¹⁰ The full set of solutions for the field orientation along the a and b axes is too lengthy and will be published in full form elsewhere.¹⁸ However, in order to understand the experimental data qualitatively some approximations can easily be made. Assuming $(B, d, K_x, K_z, M_0 H) \ll A$, the approximate solution for the magnetization can be written as

$$M_x \equiv M_0 m_x = \chi_{\perp} H_x (B + d)/d, \quad \mathbf{H} = (H_x, 0, 0), \quad (3)$$

$$M_y \equiv M_0 m_y = \chi_{\text{rot}} H_y, \quad \mathbf{H} = (0, H_y, 0), \quad (4)$$

$$M_z \equiv M_0 m_z = M_z^0 + \chi_{\perp} H_z, \quad \mathbf{H} = (0, 0, H_z), \quad (5)$$

where $M_z^0 \equiv M_s = M_0(B + d)/(A + K_z)$ is the spontaneous magnetic moment along the c axis, $\chi_{\perp} = M_0^2/(A + K_z)$ and $\chi_{\text{rot}} = M_s^2/K_z$ are the transverse and rotational susceptibilities, respectively.

Within the same approximations the frequencies of the AFMR modes in the absence of magnetic field read

$$\left(\frac{M_0}{\gamma} \omega_F\right)^2 = A K_z \frac{d}{B + d}, \quad (6)$$

$$\left(\frac{M_0}{\gamma} \omega_{AF}\right)^2 = A K_x. \quad (7)$$

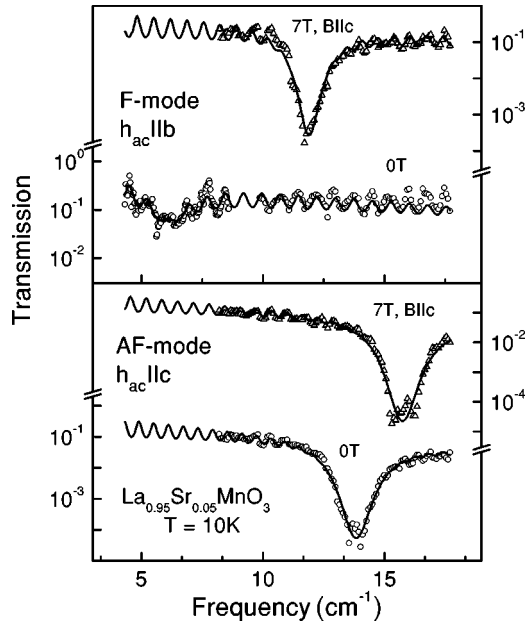


FIG. 2. Submillimeter-wave transmission spectra of single crystalline $\text{La}_{0.95}\text{Sr}_{0.05}\text{MnO}_3$ for two different geometries of the experiment at low temperatures. The lines were calculated using the Fresnel equations for the transmission of a plane-parallel plate. The behavior of the complex susceptibility was described by Eq. (1).

The analysis of Eq. (5) shows that the z axis exhibits weak ferromagnetism as the magnetization is nonzero in the absence of an external magnetic field. The magnetization along the y axis [Eq. (4)] is determined by the small rotational susceptibility and disappears in the pure antiferromagnetic case ($B=d=0$). The low-field susceptibility along the x direction [Eq. (3)] is enhanced compared to the z axis by the factor $(B+d)/d$. Qualitatively similar behavior of the magnetization is observed in Fig. 1. The solid lines in Fig. 1 were calculated using the exact expressions based on Eq. (2) and describe the experimental data reasonably well. A small static moment along the y axis appears to be strongly angle dependent and possibly is due to some residual influence of the spontaneous moment along the z axis. The absolute values of the parameters of the model were obtained by simultaneously fitting the magnetization curves and the values of the resonance frequencies in the absence of magnetic field. Despite the relatively large number of parameters in Eq. (2) (A, B, d, K_x, K_z), the requirement of a simultaneous fit allows the unambiguous determination of the parameters $A=4.67 \times 10^7$ erg/g, $B=7.4 \times 10^6$ erg/g, $K_z=3.33 \times 10^6$ erg/g, $K_x=3.42 \times 10^6$ erg/g, $d=2.1 \times 10^6$ erg/g, and $M_0=92.14$ emu/g. These parameters correspond to the average canting angle $\varphi=11^\circ$ with respect to the pure antiferromagnetic structure. From the linewidth the possible modulation of this angle may be estimated as $\pm 3^\circ$. From the values of A and K_x the interlayer exchange ($J_2=-0.37$ meV) and the single-ion anisotropy ($C=0.11$ meV) constants can be calculated¹⁰ which are in good agreement with neutron scattering data for $\text{La}_{0.95}\text{Ca}_{0.05}\text{MnO}_3$ (Ref. 20) and for $\text{La}_{0.95}\text{Sr}_{0.05}\text{MnO}_3$.⁷

Figure 2 shows the transmission spectra of the $\text{La}_{0.95}\text{Sr}_{0.05}\text{MnO}_3$ single crystal at low temperatures. The solid lines were calculated using the Fresnel equations and

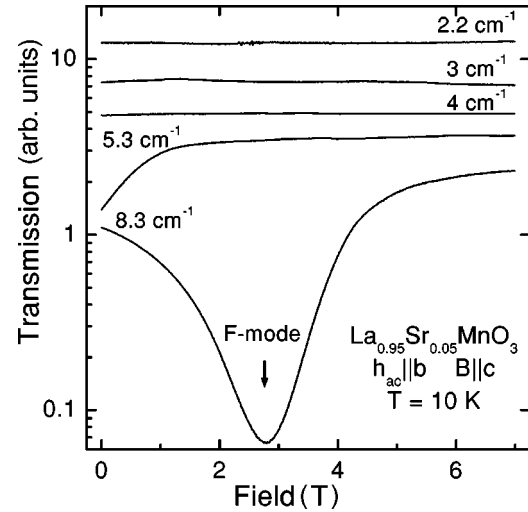


FIG. 3. Field-sweep spectra of $\text{La}_{0.95}\text{Sr}_{0.05}\text{MnO}_3$ single crystal at low temperatures. The data are scaled vertically for clarity. Due to fixed frequencies of the experiment the interference effects are not present in this arrangement.

Eq. (1) as described above. The parameters of the magnetic modes were obtained by fitting the transmission spectra. In addition, the frequency position and the appearance of the modes were also examined using field sweeps at fixed frequencies. From the data shown in Fig. 2 two peculiarities of the observed AFMR modes immediately become clear: (i) the observed lines have unique excitation conditions: $\vec{h} \parallel c$ axis for the high-frequency mode and $\vec{h} \parallel b$ axis for the low-frequency mode and (ii) no splitting of the AFMR lines is observed in finite magnetic fields for any geometry of the experiment. Both conclusions are characteristic properties of a canted antiferromagnetic structure²¹ and follow naturally from the solution of Eq. (2).

In addition, Fig. 3 represents the low-temperature transmission spectra of the $\text{La}_{0.95}\text{Sr}_{0.05}\text{MnO}_3$ single crystal in the field-sweep geometry for fixed frequencies. The interference patterns arising from the sample and from the optical elements of the spectrometer do not present within the field-sweep arrangement. This allows more clear separation and identification of different modes. However, the field-sweep experiments cannot determine the absolute intensities and are not sensitive to the modes which are weakly field-dependent. In these cases the frequency-dependent transmission is more appropriate.

The magnetic field dependencies of the resonance frequencies of both AFMR lines are shown in Fig. 4. The solid lines in Fig. 4 were calculated on the basis of the two-lattice model, discussed above. However, the parameters of the model were already fixed by fitting the magnetization curves and absolute values of the AFMR frequencies in the absence of magnetic field. Having this in mind, the theoretical curves describe the experimental data reasonably well. The most important feature of Fig. 4 is the softening of the FM mode for $B \parallel b$. This softening represents a common property of magnetic resonance in antiferromagnets and is followed by the field-induced rearrangement of the magnetic structure (spin-flop) at a critical value of magnetic field. The softening of the FM mode at low fields is in good agreement with the model calculations. The behavior for higher fields (B

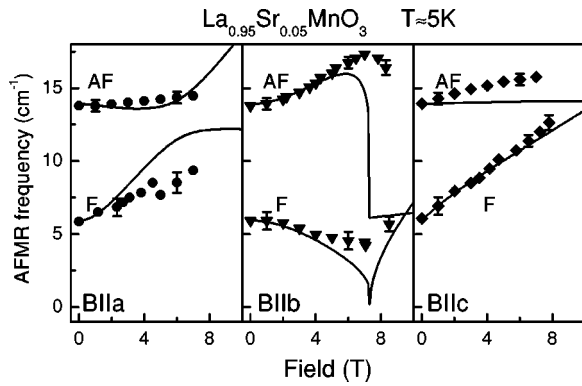


FIG. 4. Magnetic field dependence of the resonance frequencies of the AFMR lines in $\text{La}_{0.95}\text{Sr}_{0.05}\text{MnO}_3$ at low temperatures. Solid lines were calculated according to the model described in the text.

~ 7 T) significantly deviates from the model predictions. These deviations are most probably due to the extreme sensitivity of the data with respect to the exact orientation of the static magnetic field and the neglect of the higher-order terms in Eq. (2). The angular dependence of a critical behavior in a canted antiferromagnet has been calculated in details by Hagedorn and Gyorgy.¹⁹ These calculations show that already a misalignment of the magnetic field as low as one degree strongly suppresses the softening of the FM-line in the vicinity of the critical field. Most probably similar effects explain the deviations observed in Fig. 4.

Within the presented model it is also possible to calculate the absolute intensities of the AFMR modes. In the absence of static field the solution of Eq. (2) gives $\Delta\mu_{yy}=0.0080$ and $\Delta\mu_{zz}=0.0136$, using the parameters obtained above. These values are in good agreement with the experimental values $\Delta\mu_{yy}=0.012\pm 0.003$ and $\Delta\mu_{zz}=0.0120\pm 0.0010$.

Within the present model a homogeneous canted phase was assumed to explain the AFMR data. Of course, in the insulating compound $\text{La}_{0.95}\text{Sr}_{0.05}\text{MnO}_3$ the charge carriers cannot move freely, but rather form bound states. However, it has been shown by de Gennes,³ that the resulting ground state should be very close to those of free carrier model.

Finally, we discuss the possible explanation of the above-presented data within the concept of phase separation in the ferromagnetic droplets in an antiferromagnetic matrix. Already the magnetization data (Fig. 1) impose a set of constraints on the possible configuration of the phases. E.g., fer-

romagnetic moments have to be parallel to the c axis and the b axis has to be the antiferromagnetic easy axis. However, the most important consequences of a possible electronic phase separation follow for the properties of the magnetic resonances: (i) the antiferromagnetic phase would reveal an AFMR mode with a resonance frequency similar to the frequencies in pure LaMnO_3 ($\nu\sim 18\text{ cm}^{-1}$). (ii) This AFMR mode should split into two modes in the presence of magnetic field, as was observed by Mitsudo *et al.*²² in pure LaMnO_3 . (iii) A ferromagnetic line arising from the ferromagnetic droplets has to be observed. The resonance frequency of this mode should increase roughly linear with external magnetic field up to frequencies 150-250 GHz ($5-8\text{ cm}^{-1}$) for $B=7\text{ T}$.

None of these properties could be detected in the present experiment. Instead, the observed picture can be well described using the canted magnetic structure.

Assuming that the minimum detectable signal is 5% of the transmission (in the field-sweep experiment), the relative volume of the additional phases may be estimated as $\Delta V/V_0 < 0.7\%$ for the present composition.

IV. CONCLUSIONS

In conclusion, twin-free single crystals of $\text{La}_{0.95}\text{Sr}_{0.05}\text{MnO}_3$ were grown by the floating-zone method. The low-temperature magnetization was measured along the principal crystallographic directions. High field AFMR spectra of this sample were investigated in the frequency range 40–700 GHz and for magnetic fields up to $B=8$ T. Two AFMR lines having different excitation conditions were detected at low temperatures. The softening of the low-frequency mode was observed for the orientation of the static field $B||b$ and is explained by approaching to the spin-flop transition. The full data set, obtained for the $\text{La}_{0.95}\text{Sr}_{0.05}\text{MnO}_3$ single crystal, can be easily explained as arising from a canted magnetic structure and clearly contradicts the concept of phase separation into ferro- and antiferromagnetic regions.

ACKNOWLEDGMENTS

This work was supported in part by BMBF (13N6917/0 - EKM), by DFG (Pi 372/1-1), by RFBR (99-02-16849), and by INTAS (97-30850).

¹G. H. Jonker and J. H. van Santen, *Physica (Amsterdam)* **16**, 337 (1950); **19**, 120 (1953).

²E. O. Wollan and W. C. Koehler, *Phys. Rev.* **100**, 545 (1955).

³P.-G. de Gennes, *Phys. Rev.* **118**, 141 (1960).

⁴C. Zener, *Phys. Rev.* **82**, 403 (1951).

⁵E. L. Nagaev, *Sov. Phys. Usp.* **39**, 781 (1996); *Phys. Rev. B* **58**, 2415 (1998); L. P. Gor'kov, *Sov. Phys. Usp.* **41**, 589 (1998).

⁶S. Yunoki, J. Hu, A. L. Malvezzi, A. Moreo, N. Furukawa, and E. Dagotto, *Phys. Rev. Lett.* **80**, 845 (1998); S. Yunoki, A. Moreo, and E. Dagotto, *ibid.* **81**, 5612 (1998); A. Moreo, S. Yunoki, and E. Dagotto, cond-mat/9901057, *Science* (to be published).

⁷M. Hennion, F. Moussa, J. Rodriguez-Carvajal, L. Pinsard, and

A. Revcolevschi, *Phys. Rev. Lett.* **81**, 1957 (1998); M. Hennion, F. Moussa, G. Biotteau, J. Rodriguez-Carvajal, L. Pinsard, and A. Revcolevschi, *Phys. Rev. B* **61**, 9513 (2000).

⁸G. Allodi, R. de Renzi, G. Guidi, F. Licci, and M. W. Pieper, *Phys. Rev. B* **56**, 6036 (1997); G. Allodi, R. De Renzi, and G. Guidi, *ibid.* **57**, 1024 (1998).

⁹J. B. Goodenough and J.-S. Zhou, *Nature (London)* **386**, 229 (1997); P. Littlewood, *ibid.* **399**, 529 (1999).

¹⁰A. A. Mukhin, V. Yu. Ivanov, V. D. Travkin, A. Pimenov, A. Loidl, and A. M. Balbashov, *Europhys. Lett.* **49**, 514 (2000).

¹¹A. M. Balbashov, S. G. Karabashev, Ya. M. Mukovskii, and S. A. Zverkov, *J. Cryst. Growth* **167**, 365 (1996).

- ¹²A. A. Mukhin, V. Yu. Ivanov, V. D. Travkin, S. P. Lebedev, A. Pimenov, A. Loidl, and A. M. Balbashov, *JETP Lett.* **68**, 356 (1998).
- ¹³A. Urushibara, Y. Moritomo, T. Arima, A. Asamitsu, G. Kido, and Y. Tokura, *Phys. Rev. B* **51**, 14 103 (1995).
- ¹⁴G. V. Kozlov and A. A. Volkov, in *Millimeter and Submillimeter Wave Spectroscopy of Solids*, edited by G. Grüner (Springer, Berlin, 1998), p. 51.
- ¹⁵M. Born and E. Wolf, *Principles of Optics* (Pergamon, Oxford, 1986).
- ¹⁶Ch. Kittel, *Einführung in die Festkörperphysik* (Oldenburg, München, 1991) p. 528.
- ¹⁷T. Morya, in *Magnetism*, edited by G. T. Rado and H. Suhl (Academic Press, New York, 1984), Vol. I, p. 85.
- ¹⁸A. A. Mukhin *et al.* (unpublished).
- ¹⁹F. B. Hagedorn and E. M. Gyorgy, *Phys. Rev.* **174**, 540 (1968).
- ²⁰M. Hennion, F. Moussa, J. Rodríguez-Carvajal, L. Pinsard, and A. Revcolevschi, *Phys. Rev. B* **56**, 497 (1997); F. F. Moussa, M. Hennion, G. Biotteau, J. Rodríguez-Carvajal, L. Pinsard, and A. Revcolevschi, *ibid.* **60**, 12 299 (1999).
- ²¹G. F. Herrmann, *J. Phys. Chem. Solids* **24**, 597 (1963); *Phys. Rev.* **133**, A1334 (1964).
- ²²S. Mitsudo, K. Hirano, H. Nojiri, M. Motokawa, K. Hirota, A. Nishizawa, N. Kaneko, and Y. Endoh, *J. Magn. Magn. Mater.* **177-181**, 877 (1998).